Fracture 1977, Volume 1, ICF4, Waterloo, Canada, June 19 - 24, 1977

THE IMPACT TESTING OF POLYMERS - A REASSESSMENT

J. G. Williams* and M. W. Birch*

ABSTRACT

The elastic analysis of the conventional impact test is presented and it is shown that for unstable failures the energy absorbed must be expressed as a particular function of crack length, ϕ, rather than the conventional ligament area, if values of G_c are to be deduced. It is further shown that the conventional corrections for plasticity effects and plastic collapse analyses may be applied to the data. In addition, kinetic energy effects are examined and suitable corrections suggested. Experimental data for several polymers is given which shows that unstable failures only are observed and that both small and large scale plasticity effects occur in polymers.

INTRODUCTION

Polymers are particularly susceptible to brittle fracture when subjected to impact loading. Materials which give tough behaviour at low speeds frequently exhibit brittle failure under impact conditions and naturally this has led to an emphasis on impact testing in the plastics industry. The conventional Charpy and Izod pendulum tests have been taken over from metals testing in a suitably scaled down form. Of the two, the Izod test is by far the most popular and the "Izod Number", the energy absorbed in fracturing a standard dimensioned specimen, is the most widely used mechanical property in plastics testing.

It is usually appreciated, however, that the test and the interpretation of the data, is subject to considerable limitations. There is, for example, only limited correlation between Charpy and Izod results and there is no direct way of using the data in component design (for a comprehensive review see [1]). The numbers obtained are known to be dependent on specimen size which makes their use in design uncertain. Part of this difficulty arises from using only a single specimen geometry but in addition the practice of measuring the energy to failure is regarded as unsatisfactory.

The use of energy to describe impact failures is clearly dictated by convenience but there are uncertainties since one is measuring the sum of several possible effects and much information is inaccessible. The desirable procedure of measuring loads during fracture has therefore been pursued by many workers (e.g., [2],[3]), both from a simple desire to extract more information from a test and, more specifically, for use in fracture mechanics calculations. The difficulties are considerable and stem mainly from the loading times being comparable with those for stress waves to traverse the specimen. This results in severe distortion of the

*Department of Mechanical Engineering, Imperial College of Science and Technology, Exhibition Road, London SW7 2BX, England.

recorded loads so that very large corrections are necessary to arrive at any measure of fracture load. In addition, the experiments require expensive equipment and skilled operators and are unsuitable for routine work.

There is scope for a re-appraisal of the situation since there has been some success in applying fracture mechanics to the conventional energy measuring test [4,5,6,7]. This idea will be developed here together with methods for coping with plasticity effects during fracture. In addition, some consideration will be given to the problem of correcting data for kinetic energy effects, which bedevil the testing of low strength materials.

LINEAR ELASTIC THEORY [8]

It will be assumed initially that impact failures may be described in terms of linear elasticity so that when a load P is applied to a specimen containing a crack of area A (see Figure 1(a)), a deflection Δ is produced such that:

$$\Delta = CP \tag{1}$$

where C is the compliance of the specimen and is constant for a given crack area. Thus, there is a linear load deflection curve as shown in Figure 1(b). Suppose now that the crack grows by a small area δA and the load changes by δP and the deflection by $\delta\Delta$. The initial stored elastic energy is given by:

$$U_1 = \frac{1}{2} P \Delta$$

and the final stored energy by:

$$U_2 = \frac{1}{2} (P + \delta P)(\Delta + \delta\Delta)$$

In addition, there is external work performed given by:

$$W = \left(P + \frac{\delta P}{2}\right) \delta\Delta \tag{2}$$

The net energy released by the system is therefore:

$$\delta U = W + U_1 - U_2$$

and substituting for W, U_1 and U_2, we have:

$$\delta U = \frac{1}{2} (P\, \delta\Delta - \Delta\, \delta P) \tag{3}$$

There will be a change in C because of A changing by δA, so from equation (1):

$$\delta\Delta = C\, \delta P + P\, \delta C \tag{4}$$

By combining equations (1), (3) and (4) we have two results for the energy release rate per unit area:

$$\frac{dU}{dA} = \frac{1}{2} P^2 \cdot \frac{dC}{dA} = \frac{1}{2} \frac{\Delta^2}{C^2} \cdot \frac{dC}{dA} \tag{5}$$

Notice that these results are independent of either load or displacement change.

If fracture occurs when:

$$\frac{dU}{dA} = G_c \tag{6}$$

then G_c may be determined for a given test if C is known as a function of A (and hence dC/dA) when either P or Δ are determined at fracture. Clearly, this is an instantaneous condition since it refers to the current loads and deflections. If it is assumed that G_c remains constant throughout the crack growth then clearly dU/dA must be maintained at G_c throughout. If a crack grows from area A_1 to area A_2 under this condition, then the total energy required is:

$$U = G_c (A_2 - A_1) \tag{7}$$

If a crack is propagated under these conditions in an impact test then, assuming that the machine measures the energy absorbed by the fracture, the conventional procedure of estimating G_c by:

$$G_c = \frac{U}{A_2 - A_1}$$

will give a satisfactory result.

While G_c must be maintained throughout crack growth, this total energy condition will not always hold. If, at crack initiation, dU/dA can be maintained at G_c at constant displacement, then the crack will propagate without the addition of external work so that the energy absorbed is that stored in the specimen at initiation, i.e.,

$$U_1 = \frac{1}{2} P \Delta = \frac{1}{2} P^2 C$$

and from equation (5):

$$U_1 = G_c \left(\frac{C}{dC/dA}\right) = G_c \cdot \Omega \tag{8}$$

The constant displacement, or unstable condition, will pertain until it can no longer be sustained at which time external work must be imparted resulting in stable crack growth thereafter. A criteria for instability may be obtained from equation (5) in that a crack will be unstable if:

$$\frac{d^2U}{dA^2} > 0 \text{ at } \frac{dU}{dA} = G_c \tag{9}$$

with the limiting condition of $d^2U/dA^2 = 0$. If this is to be sustained at constant deflection, then from equation (4):

$$\frac{1}{P} \cdot \frac{dP}{dA} = -\frac{1}{C} \cdot \frac{dC}{dA}$$

and from equation (5);

$$\frac{d^2U}{dA^2} = P^2 \left[\frac{1}{2} \frac{d^2C}{dA^2} - \frac{1}{C} \left(\frac{dC}{dA}\right)^2\right]$$

For $P \neq 0$ the crack will be unstable for:

$$\frac{1}{2}\,\frac{d^2C/dA^2 .\ C}{(dC/dA)^2} > 1$$

From equation (8) we may introduce the function Ω and the condition becomes:

$$\frac{d\Omega}{dA} < -1 \qquad (10)$$

(i.e. the energy released $G_c\, d\Omega > G_c\, dA$ that absorbed).

Three conditions are feasible using this criterion as shown in Figure 2:

1. Here the crack is always stable and $d\Omega/dA > -1$ at all times. The stored energy at initial crack growth (the shaded area) is augmented throughout by external work to give the required work $G_c\,(A_2 - A_1)$.

2. In this condition $d\Omega/dA < -1$ throughout propagation and the crack is completely propagated by the stored energy. In this condition $G_c\,\Omega > G_c\,(A_2 - A_1)$ and the conventional procedure of determining G_c from $U/(A_2 - A_1)$ is not valid and should be replaced by W/Ω.

3. $d\Omega/dA = -1$ at some condition during unstable growth and crack arrest will result. Subsequent external work must be supplied to effect propagation so that finally $U = G_c(A_2 - A_1)$ as in the fully stable case.

It should be noted that the limiting condition $d\Omega/dA = -1$ is equivalent to a total energy balance for a constant G_c case, since by integration:

$$\Omega = -A + H \qquad \text{(H is a constant)}$$

Thus, the total energy, U_1:

$$U_1 = G_c\,\Omega = G_c\,(-A + H)$$

For full propagation $A = A_1$ for $\Omega = \Omega_1$ and $A = A_2$ for $\Omega = \Omega_2$, and hence,

$$U = G_c\,(\Omega_1 - \Omega_2) = G_c\,(A_2 - A_1)$$

i.e., the condition $d^2U/dA^2 = 0$ is identical to that of:

$$(\Omega_1 - \Omega_2) = (A_2 - A_1) \qquad (11)$$

THE CHARPY TEST

The consequences of these general concepts will now be applied to the particular geometry of the Charpy test shown in Figure 3. (Although the Izod test is more widely used, it is considered to be basically inferior to the Charpy because of clamping effects). If the crack length is a, then the crack area is:

$$A = B\,a$$

which may be conveniently non-dimensionalized as:

$$\frac{A}{B\,D} = \frac{a}{D} = x$$

The energy required to propagate a crack from x_1 to x_2 is therefore:

$$U = G_c\,B\,D\,(x_2 - x_1)$$

The initiation condition may be written in terms of:

$$\Omega = \frac{C}{dC/dA} = B\,D\,\frac{C}{dC/dx} = B\,D\,\phi$$

so that equation (11) becomes:

$$\phi_1 - \phi_2 = x_2 - x_1$$

i.e., $$\phi_1 + x_1 = \phi_2 + x_2 \qquad (12)$$

ϕ has been computed for the Charpy goemetry [6] for various L/D ratios and these are shown in Figure 4 plotted as $\phi + x$ as a function of x (the broken lines are extrapolations of numerical data). For complete fracture of the specimen, $x_2 = 1$ and $\phi_2 = 0$ and hence for complete instability we have:

$$\phi + x > 1$$

and this condition is shown in Figure 5 as the value of x as a function of L/D. For $\phi + x < 1$ there are some values for which there are two possible x values which corresponds to the crack arrest case. The limit of this is the minimum point and for x greater than this, the cracks are always stable. These minima are also shown as a function of L/D in Figure 5. The solution for the small crack case (the Griffith solution) is also shown, i.e.,

$$\phi = \frac{1}{2}\,x + \frac{1}{18\pi}\left(\frac{L}{D}\right)\frac{1}{x}$$

to give the short crack values. Figure 5 is marked with the three regions of behaviour.

If the energy to failure U is plotted as a function of $BD\phi$ and if unstable behaviour pertains, a straight line should result as shown. If stable crack growth is occurring, then U will be linear with $BD\,(1 - x)$ and not $BD\phi$ in Figure 6. Figure 6 shows the type of curve expected if stable data is plotted as a function of ϕ. Clearly, there is pronounced non-linearity for high ϕ values but initially (i.e. for $x \rightarrow 1$) a reasonably straight line is produced.

PLASTICITY EFFECTS

The extent of the plastic zone at the tip of a crack at fracture can be estimated from:

$$r_p = \frac{\pi}{8}\,\frac{E\,G_c}{\sigma_y^{\,2}} \qquad (13)$$

assuming that the zone is a line-like extension of the crack. Here E is the Young's modulus of the material and σ_y the yield stress. Since this analysis is conducted in terms of energy it is preferable to use the energy per unit volume to produce yielding in plane stress in an elastic material:

$$w_p = \sigma_y^2/2E$$

Equation (13) now becomes:

$$r_p = \frac{\pi}{16}\frac{G_c}{w_p} \qquad (14)$$

This zone distorts the elastic stress field but its effect may be modelled in practice by changing a to a + r_p providing that $r_p < a$. It is difficult to estimate r_p in impact since w_p is not known for these conditions but the effect may be modelled by considering the influence of the addition of various r_p/D values to the x used to determine ϕ. Figure 7 shows this data for L/D = 6 and the non-linear effects are apparent at the higher (> 1) ϕ values. Note also that reasonably linear lines occur at low ϕ values giving fictitious G_c values. This form of non-linearity persists in a plot against (1 - x) and can only be corrected by plotting against revised values using guessed r_p values to achieve linearity.

The broken line in Figure 7 represents the condition for the onset of general yielding in the specimen and may be estimated as:

$$x \leq \frac{r_p}{D}$$

For x > 0.5 there is clearly no solution for $r_p/D = 0.5$. For smaller crack lengths than the critical condition, the specimen undergoes large scale yielding which may be modelled by the limiting case of a fully developed plastic hinge at the cracked section. The load necessary to produce the hinge is:

$$P_p = \sigma_y \frac{BD^2}{L} (1 - x)^2$$

If rigid rotation of the specimen about the hinge is assumed, then the displacement at the crack tip is:

$$u = \frac{2D}{L}(1 - x)\Delta$$

If we now extend the line plastic zone concept to the fully plastic case we may write:

$$G_c = u\,\sigma_y$$

and since the work necessary to give u is:

$$U_p = P_p \Delta$$

then $$U_p = G_c B D \cdot \frac{1}{2}(1 - x) \qquad (15)$$

This is the fully plastic solution involving no elasticity effects and is appropriate to the condition for $r_p/D > 0.5$ and x > 0.5. This test state

has been advocated for metals using the J_c analysis [9]. When less extensive plasticity is involved with short crack lengths, then the energy input to achieve G_c is made up of an elastic and a plastic part. If $\phi = \phi_p$ for $x = r_p/D$, then for $x < r_p/D$ the energy relationship is:

$$\frac{U}{BD\,G_c} = \frac{1}{2}(1 - x) + \frac{\phi_p}{\phi}\left[\phi - \left(\frac{1 - x}{2}\right)\right]$$

In fact, this function does not distort the corrected plot greatly and is unlikely to be seen effectively in experimental data.

All the preceding comments on plasticity effects have assumed that the fracture is unstable. If stable growth occurs, then an identical relationship to the elastic case pertains.

SUMMARY OF DATA ANALYSIS

The analysis of impact data depends critically on establishing whether propagation is stable or unstable. If instability is assumed, then the crack once initiated will proceed to complete failure implying, in general, that the propagation G_c is less than the initiation value. Data must then be plotted as U verses ϕ to determine G_c. If plasticity effects occur, non-linearity is evident in this plot and can be corrected by the addition of a plastic zone correction factor to ϕ. Large scale plastic deformation cannot be corrected by this method but for a full plastic hinge, a G_c can be determined from a ligament area calculation because of the low elastic energy contribution.

If the crack propagation can be stable and occurs, for example, at a constant G_c, then only very short crack lengths give unstable growth and generally the data must be analyzed as U as a function of ligament area. This relationship is not dependent on elastic behaviour and includes plasticity effects. There is some scope for confusion with a fully plastic, unstable case since only a factor of two differentiates them, but comparison with limiting values in the U versus $BD\phi$ graph should clarify the situation.

KINETIC ENERGY EFFECTS

The preceding discussion has assumed that the measured energy corresponds to that absorbed by the specimen either in stored elastic energy or by propagating the fracture. In practice, however, some is absorbed in the form of kinetic energy and may be an appreciable quantity at impact speeds. Since the impact strength is defined for high rates, then it is arguable that a kinetic energy term is a necessary part of effective fracture toughness and need not be removed. It turns out, however, that the kinetic effects are dependent on specimen size and if realistic estimates of energies necessary to cause impact failures are to be made, then it must be possible to separate the fracture work from the kinetic terms. This is not a simple matter since it is difficult to compute or measure kinetic energy with any precision. Some useful results may be obtained, however, by considering simple models of the impact process as a guide to phenomena expected in the test.

RIGID BODY IMPACT

Consider the impact test to be modelled by a large striker of mass M impinging on a small specimen of mass m whose stiffness can be represented by a spring of compliance C. If the two masses are considered as rigid bodies, then from momentum:

$$M V + m V_o = M V_1 + m V_2 \qquad (16)$$

where V, V_1 are the initial and final velocities of M, respectively, and V_o and V_2 are those for m. If the Newtonian concept of a coefficient of restitution e is invoked, then:

$$e = \frac{V_2 - V_1}{V - V_o} \qquad (17)$$

If $\alpha = m/M$, then by combining equations (16) and (17), we have:

$$V_1 = V\left(\frac{1 - \alpha e}{1 + \alpha}\right) + V_o \alpha \left(\frac{1 + e}{1 + \alpha}\right)$$

and

$$V_2 = V\left(\frac{1 + e}{1 + \alpha}\right) - V_o \left(\frac{e - \alpha}{1 + \alpha}\right) \qquad (18)$$

For most impact tests $\alpha << 1$, and the equations become:

$$V_1 = V \text{ and } V_2 = (1 + e) V - e V_o \qquad (19)$$

The energy lost by the striker is:

$$U_1 = \frac{1}{2} M (V^2 - V_1^2) = m V^2 (1 + e) (1 - \frac{V_o}{V}) \qquad (20)$$

and the energy of the specimen is:

$$U_2 = \frac{1}{2} m (V_2^2) = \frac{1}{2} m V^2 (1 + e (1 - \frac{V_o}{V}))^2 \qquad (21)$$

After impact, the kinetic energy of the specimen, U_2, is converted to strain energy in the spring. For a deflection of Δ the stored energy is $1/2 \ \Delta^2/C$ so that we may write:

$$U_2 = \frac{1}{2} m \dot{\Delta}^2 + \frac{1}{2} \frac{\Delta^2}{C}$$

and differentiating again:

$$0 = \dot{\Delta} (\ddot{\Delta} + w^2 \Delta) \quad \text{where } w^2 = (mC)^{-1}$$

and the solution is:

$$\Delta = \frac{V_2}{w} \sin wt \qquad (22)$$

On the first impact $V_o = 0$ and $V_2 = (1 + e) V$ so that the specimen leaves the striker, compresses the spring, and then as the spring recovers, makes the second impact with the striker as sketched in Figure 9. The time of the second impact, t_1, is given by:

$$wt_1 = (1 + e) \sin wt_1 \qquad (23)$$

and the velocity:

$$V_o = V (1 + e) \cos wt_1 \qquad (24)$$

The process is then repeated with the new V_o value and hence a new t_1 is determined.

Clearly, the nature of this effect depends on e and the behaviour it implies. For $e = 0$ we have perfectly plastic impact and $V_2 = V$ for all V_o values and there is no bouncing since the specimen continues with the striker and:

$$U_1 = m V^2 \text{ and } U_2 = \frac{1}{2} m V^2$$

Here $1/2mV^2$ is lost on the first impact but $U_1 = U_2 + 1/2mV^2$ thereafter. The other extreme case is perfectly elastic impact with no loss in which $e = 1$. Here $V_2 = 2V$ for the first impact and $U_2/U_1 = 1$. The situation in subsequent impacts is shown in Table I and since V_o is negative, there is an increase in the relative velocity at impact and more energy is impacted at each blow as shown in the U_1 values. Also shown in Table I are some values for $e = 0.3$ where V_o is positive so that the relative velocities decrease finally resulting in $V_2 < V$ and the specimen is carried along by the striker. There is a critical value of $e = (\pi/2 - 1)$ which results in $V_o = 0$ and in all cases the impacts are identical with $V_2/V = \pi/2$, $wt_1 = \pi/2$, and $U_1 = 1/2mV^2\pi$.

If bouncing is occurring, then the energy measured is in units, or quanta, which depend on e. Some of this energy (for $e < 1$) will then go into strain energy and during some bounce phase the specimen will fracture. The measurements will never be able to discriminate more accurately than the current quantum which has been imparted. For example, in Table I values for $e = 0.8$ are computed and the U_1 values will be the measured quanta. Some of this energy is stored in elastic deformation, some is returned during the next impact as kinetic energy and some is lost.

DETERMINATION OF G_c

To determine G_c experimentally, a graph of the energy absorbed U_1 must be plotted against either $BD\phi$ or ligament area A so that G_c may be derived from the slope of the resulting straight line. Assuming now that one or other of these representations is appropriate, then either may be regarded as proportional to the energy stored elastically, U_2. Figure 10 shows the general nature of the expected result with the data falling in bounds because of the kinetic energy effects and bouncing. The calculations are for three values of e and clearly $e = 1$ forms bounds for the other cases. The lower bound is the desired result of $U_1 = U_2$ while the upper bound corresponds approximately to $U_1 = 1.5 \ U_2$. The increasing quântum effect is also apparent in this and the $e = 0.8$ case. The interval for $e = 0.57$ is constant and the average line through this data has an intercept of $U_1 = \pi/2 \ (1/2mV^2)$ and a slope of $U_1 = 4/\pi.U_2$. If it is assumed that the data lie within the range $1/3 < e < 1$, then this line will represent a reasonable average to the results. The measured slope can be corrected by a factor of $\pi/4$ which, of course, assumes that the energy lost in stress waves is indeed lost and is not available for fracture.

Some inherent limitations of the test are apparent from this analysis. The elastic bouncing phenomenon means that there is an inherent discrimination phenomenon which may be expressed as:

$$U_2 > 2\,m\,V^2 \qquad (25)$$

Assuming an unstable form of fracture, this may be written in terms of a factor f such that:

$$f = \frac{1}{2}\frac{G_c \phi}{L\,\rho\,V^2} \qquad (26)$$

To obtain useful data, f must be greater than about 2 which means that for low G_c values, it may be necessary to use low L values and in extreme cases V may have to be reduced.

The discussion here has been directed towards simple energy measurements and clearly more information is obtained if load measurements are taken. If the striker is instrumented, however, the same problems exist in that pulses of load will be recorded with the same uncertainties as in the energy measurements. Instrumented specimens do provide much more information but are expensive to use, particularly since it may be necessary to take several measurements to establish the deformation pattern in the specimen. It seems unlikely that such a method could be used on any regular testing basis and since no particular advantage is obtained by instrumenting the striker, the conventional energy measurement seems the most desirable. The device of reducing the contact stiffness to avoid bouncing is of dubious value since it introduces the additional uncertainty of contact point losses which must be corrected.

SOME EXPERIMENTAL OBSERVATIONS

There has been a substantial body of information which shows that the concepts outlined here work reasonably well in practice [4,5,6,7] but not a great deal on the details of thes tests. Some data is given here which illustrates some of the factors involved.

DETERMINATION OF e

A series of tests were performed in which unrestrained specimens were knocked off the supports of a pendulum impact testing machine and the energy recorded. Four materials were tested, namely polymethylmethacrylate (PMMA), polytetrafluoroethylene (PTFE), medium density polyethylene (MDPE) and a thermoset resin, and the length/depth ratio was varied between 5 and 10. The data is shown in Figure 11 and is remarkably consistent giving an average value of e of 0.53. Each point represents an average of five readings and the scatter was never more than 5%. No trend with specimen mass or dimensions is discernible.

e is not a material property but reflects such parameters as contact stiffness and specimen size and shape. Apparent e values have been computed for different simple geometries (e.g. [10],[11]) in terms of stress wave interactions and illustrate clearly that the energy "loss" implied in e is more accurately regarded as a measure of energy distribution for the size and shape of specimen and striker, and the time scale of the test. Some energy is undoubtedly lost in plastic dissipation at the contact point but the majority of the apparent loss is in the form of stress waves moving

through the specimen. It is not surprising, therefore, that the data are so similar for the various materials since they reflect the similar dimensions of the specimens more strongly than they do the material properties. The value of $e \simeq 0.5$ gives a moderate intrinsic scatter on the data (see Figure 10) but does imply that the G_c value obtained from the slope should be corrected by a factor of 3/4 to remove kinetic effects. For comparison purposes, this is not important since it is the same for all materials and some kinetic energy distribution effect is an essential part of the fracture toughness under impact conditions. Care should be taken, however, to quantify the kinetic energy effect with substantial size changes.

FRACTURE DATA

Figure 12 shows some data obtained for PMMA Plotted as U versus $BD\phi$ (ϕ taken from reference [6]) and a good straight line is indicated. The intercept is the measured kinetic energy from unsupported specimens. The measured slope G_c value is 1.05 kJ/m^2 which gives an absolute value of 0.81 kJ/m^2. Data of this type is obtained from moderately tough, glassy polymers in which the toughness to density ratio is such as to present no problems from discrimination effects.

Figure 13 shows some satisfactory data for a considerably tougher glass fibre reinforced thermoset resin. There is more scatter in the data because of the nature of the material but there is sufficiently good linearity to obtain a value of G_c.

Figure 14 shows data for a moulding compound of rather high density and low toughness. The results for the 41 mm span and 3.36 m/s velocity show considerable scatter and no trend with all the values in fact less than the kinetic energy reading. On reducing the span to 21 mm there is some improvement but it is only when the velocity is decreased to 2.44 m/s with a 21 mm span that a good line is obtained. The f factor (equation (26)) is shown on the figure for the three cases and as expected $f \simeq 2$ is required to give a satisfactory result.

Some results on a medium density polyethylene shown in Figure 15 illustrate the influence of plasticity effects. There is a distinct curvature in the U versus $BD\phi$ data and when this is plotted as U versus ligament area in Figure 16, there is again distinct curvature, this time in the opposite direction. When plastic zone correction factors are applied to Figure 15, however, it can be seen that r_p = 0.5 mm gives very good linearity and G_c = 14.2 kJ/m^2. The use of r_p = 1 mm clearly over-corrects the data.

An example of a more pronounced plasticity effect is shown in Figure 17 which gives data for an acrylobutadienestyrene (ABS) resin. The curvature in this energy versus $BD\phi$ graph is very pronounced tending to a limiting value at high ϕ (small a) values. When plotted on a ligament area basis in Figure 18, this gives a good straight line. Assuming that this is a plastic collapse situation, then G_c may be computed from equation (15), i.e. $G_c = 2U/A$ giving 23 kJ/m^2. This slope is shown on the $BD\phi$ graph in Figure 17 and it is a reasonable assumption that plasticity corrections to would give such a value. Simply adding an r_p correction to a is, of course, not possible in this case since r_p is large. The horizontal line is the fully plastic collapse energy for x = 0.

CONCLUSIONS

The analysis of the impact test presented here has illustrated the wide range of possibilities in the data. Conditions for stable and unstable failure, plastic deformation effects and finally kinetic energy phenomena all play a part. Only the latter, however, presents a fundamental difficulty since the inclusion of corrections is problematical even if they can be made. The other effects can be established by careful observation of the variation of absorbed energy with crack length.

While many possibilities exist, in practice the situation turns out to be relatively simple. The energy loss factor (e) is essentially constant and kinetic energy effects are seen in all tests as a positive energy intercept. Stable crack growth data giving a constant propagation energy has not been observed in these tests (and presumably this implies that in most polymers the propagation G_c is less than the initiation value). Materials with small plasticity effects (the glassy polymers) give very good energy versus $BD\phi$ lines and the tougher materials which show plasticity effects seem to be amenable to plastic zone correction factors. Materials which are deliberately designed to absorb energy by yielding, such as ABS, seem to be amenable to description in terms of a full plastic collapse of the cracked section. Thus, the careful application of conventional fracture mechanics techniques to the simple energy impact test can elevate the results from doubt and uncertainty to the point of giving reliable information.

ACKNOWLEDGEMENT

The authors wish to thank Miss L. V. Maxwell for the data given in Figures 17 and 18, and Dr. G. P. Marshall for that in Figure 12.

REFERENCES

1. VINCENT, P.I., Plastics Institute Monograph, 1971.
2. RICHARD, K., J. Polym. Sci., 58, 1962, 71.
3. RADON, J.C., and TURNER, C.E., Eng. Fract. Mechs., 1, 1969, 411.
4. MARSHALL, G.P., TURNER, C.E. and WILLIAMS, J.G., J. Mater. Sci., 8, 1973, 949.
5. BROWN, H.R., J. Mater. Sci., 8, 1973, 941.
6. PLATI, E. and WILLIAMS, J.G., Polym. Eng. Sci., 15, 1975, 470.
7. PLATI, E. and WILLIAMS, J.G., Polymer, 16, 1975, 915.
8. GURNEY, C. and HUNT, J., Proc. R. Soc., A299, 1967.
9. RICE, J.R., PARIS, P.C. and MERKLE, J.G., ASTM, STP 536, 1973, 231.
10. JOHNSON, W., Impact Strength of Materials, E. Arnold, 1972.
11. TOMOSHENKO, S.P. and GOODIER, J.N., Theory of Elasticity, McGraw-Hill, 3rd ed., 1970, 420.

TABLE I

Impact Number	V_2/V	ωt_1	V_o/V	$U_1/\frac{1}{2}mV^2$	
1	2.00	1.89	- 0.64	4.00	e = 1.0
2	2.64	2.16	- 1.48	6.56	
3	3.48	2.38	- 2.52	9.92	
4	4.52	2.55	- 3.77	14.08	
5	5.77	2.66	- 5.11	19.08	
1	1.80	1.78	- 0.37	3.60	e = 0.8
2	2.10	1.92	- 0.72	4.95	
3	2.37	2.07	- 1.13	6.18	
4	2.70	2.19	- 1.57	7.67	
1	1.30	1.22	0.44	2.60	e = 0.3
2	1.17	0.98	0.65	1.46	
3	0.97				
All	$\pi/2$	$\pi/2$	0	π	e = ($\pi/2$ - 1)

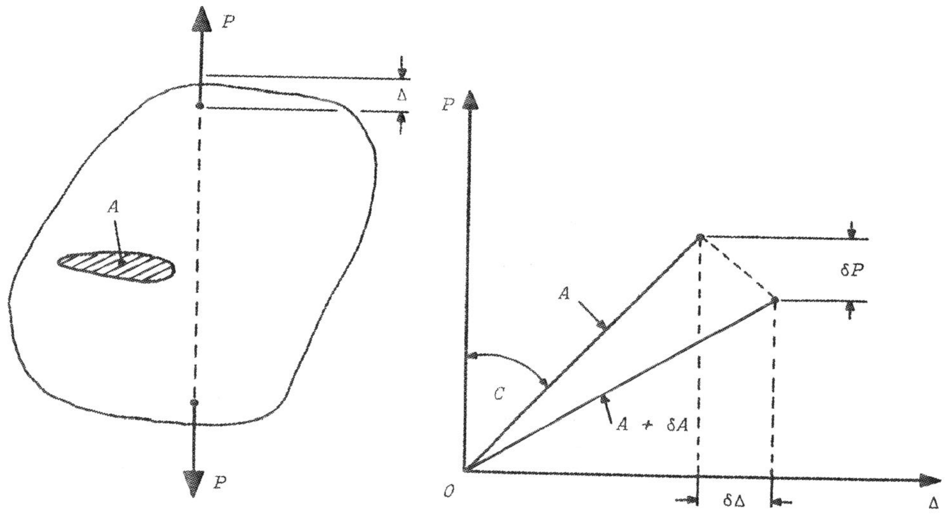

(a) Geometry (b) Loading diagram

Figure 1 Linear elastic cracked body

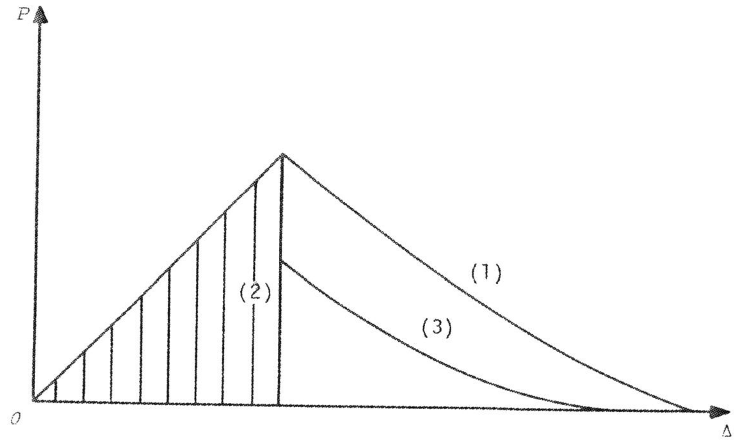

Figure 2 Load deflection diagram for:
(1) Stable fracture;
(2) Unstable fracture;
(3) Unstable fracture with arrest

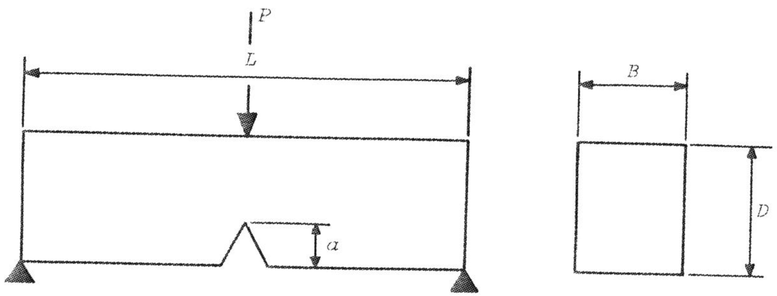

Figure 3 Charpy test geometry

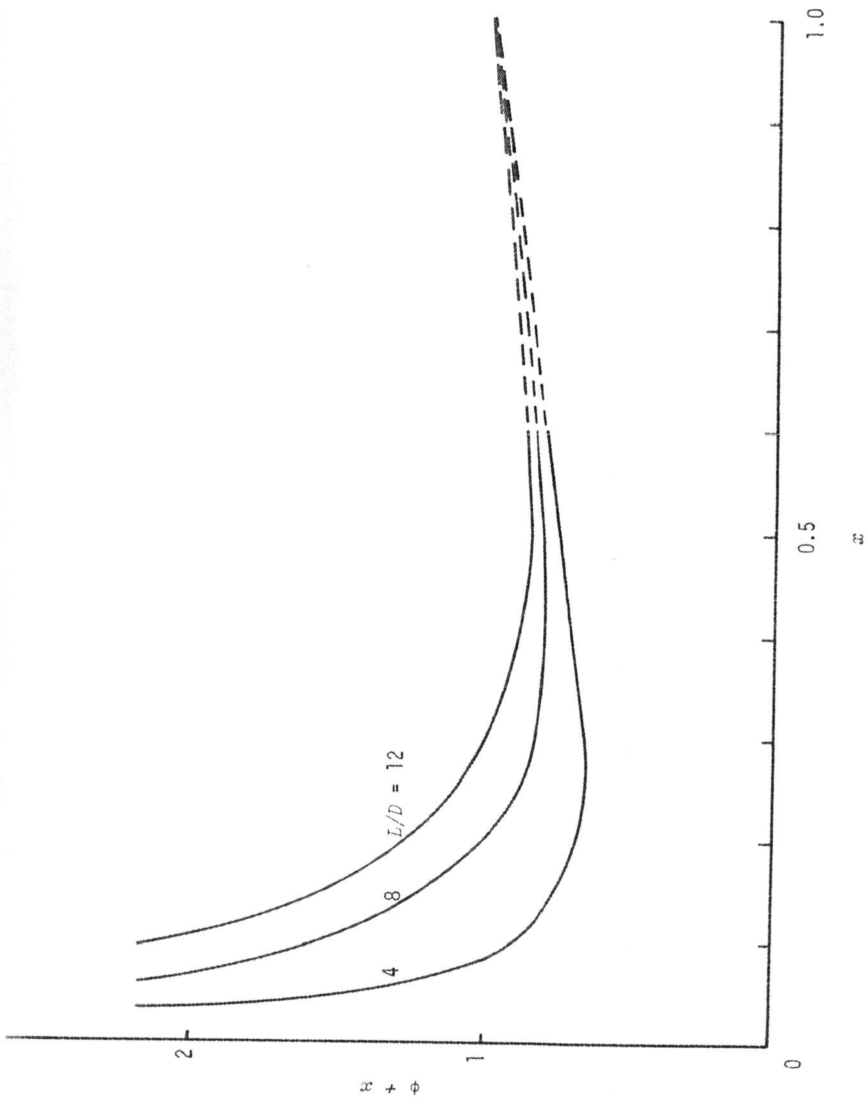

Figure 4 Stability function for Charpy geometry

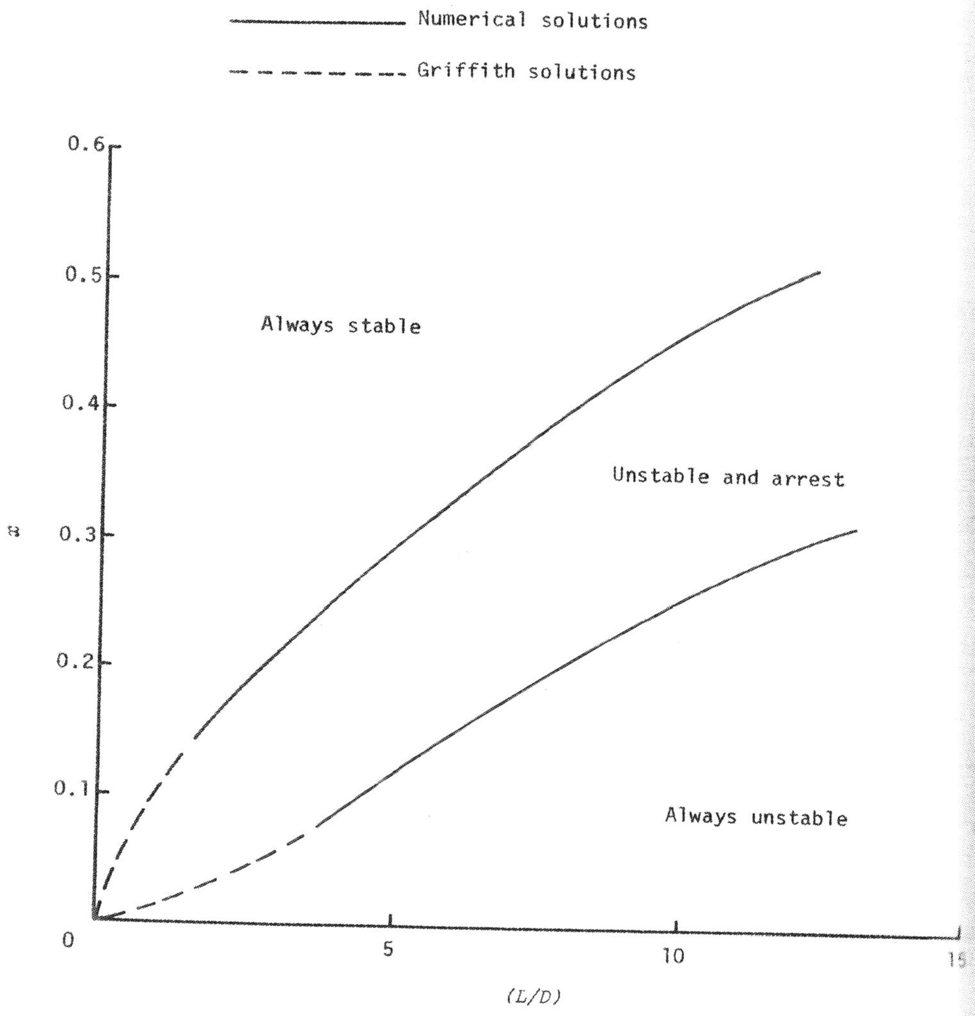

Figure 5 Stability regions for the Charpy test

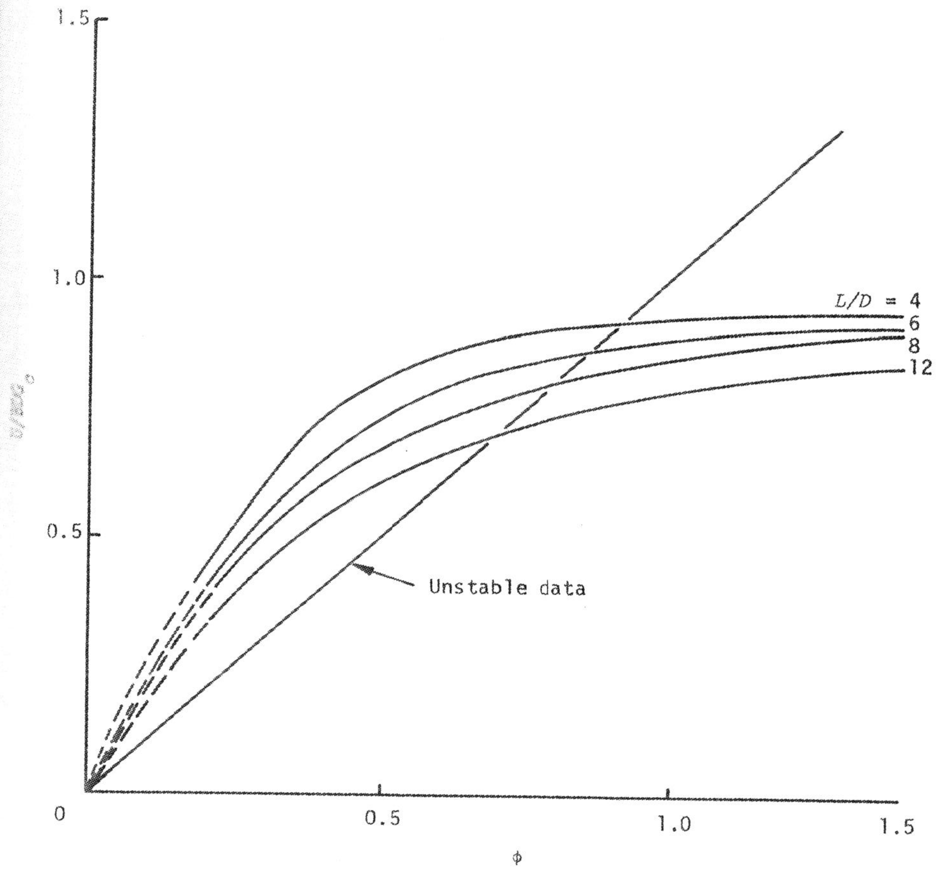

Figure 6 Stable crack growth plotted on an unstable crack basis

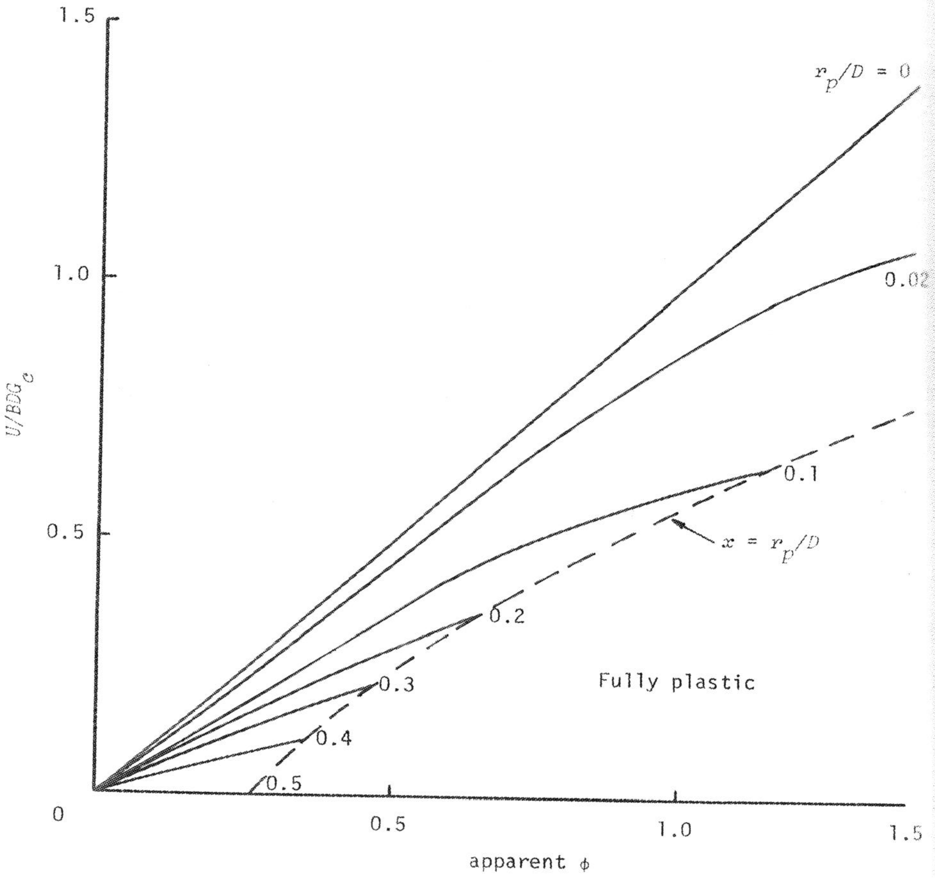

Figure 7 The effect of a plastic zone on unstable data

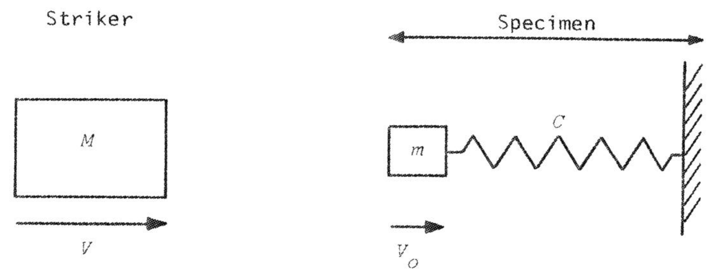

Figure 8 Rigid body model of impact

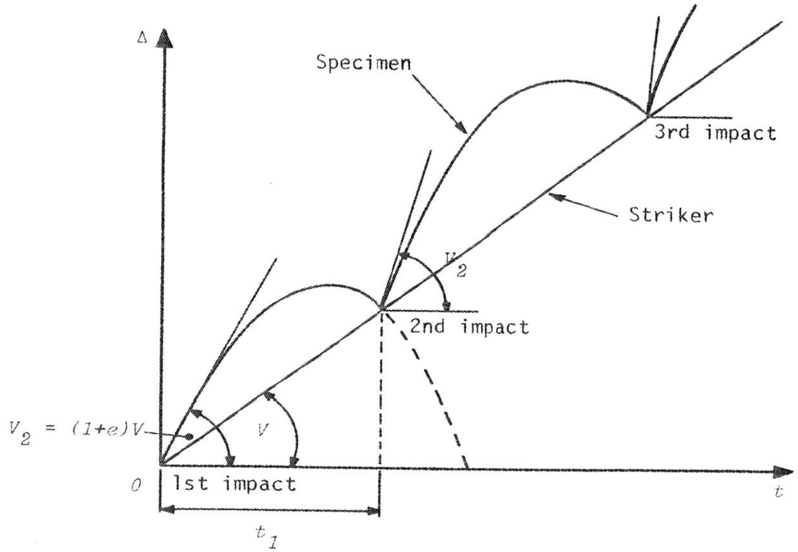

Figure 9 Schematic representation of impact behaviour

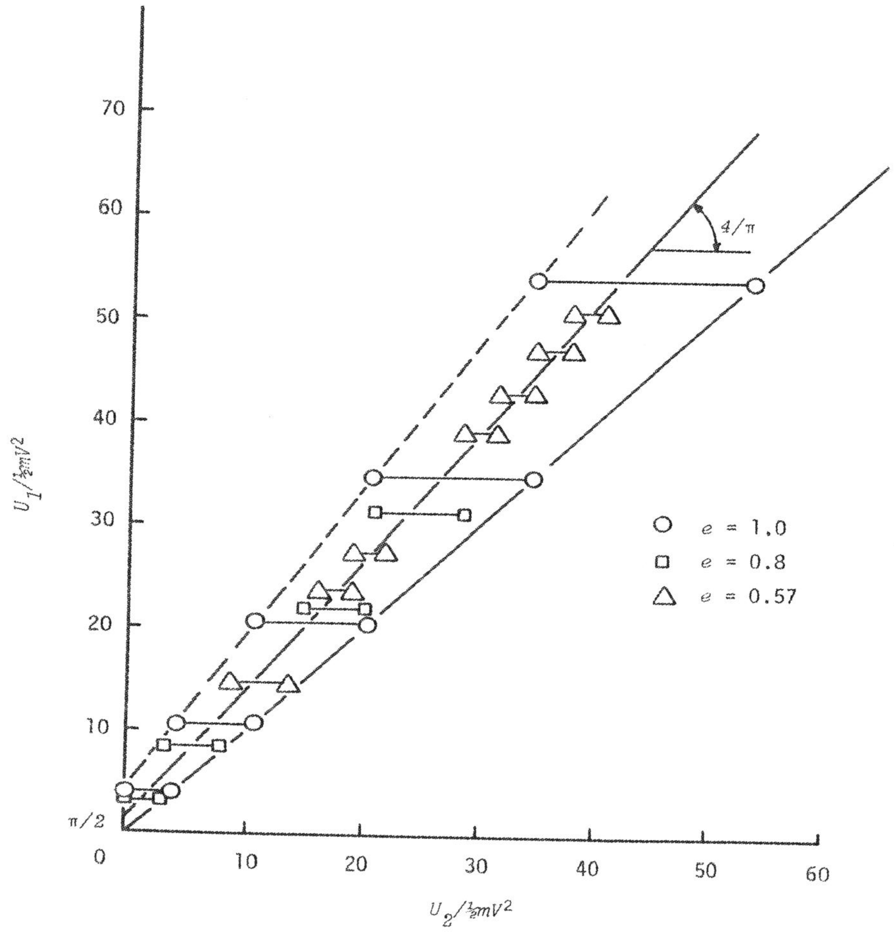

Figure 10 Measured energy as a function of energy in the specimen

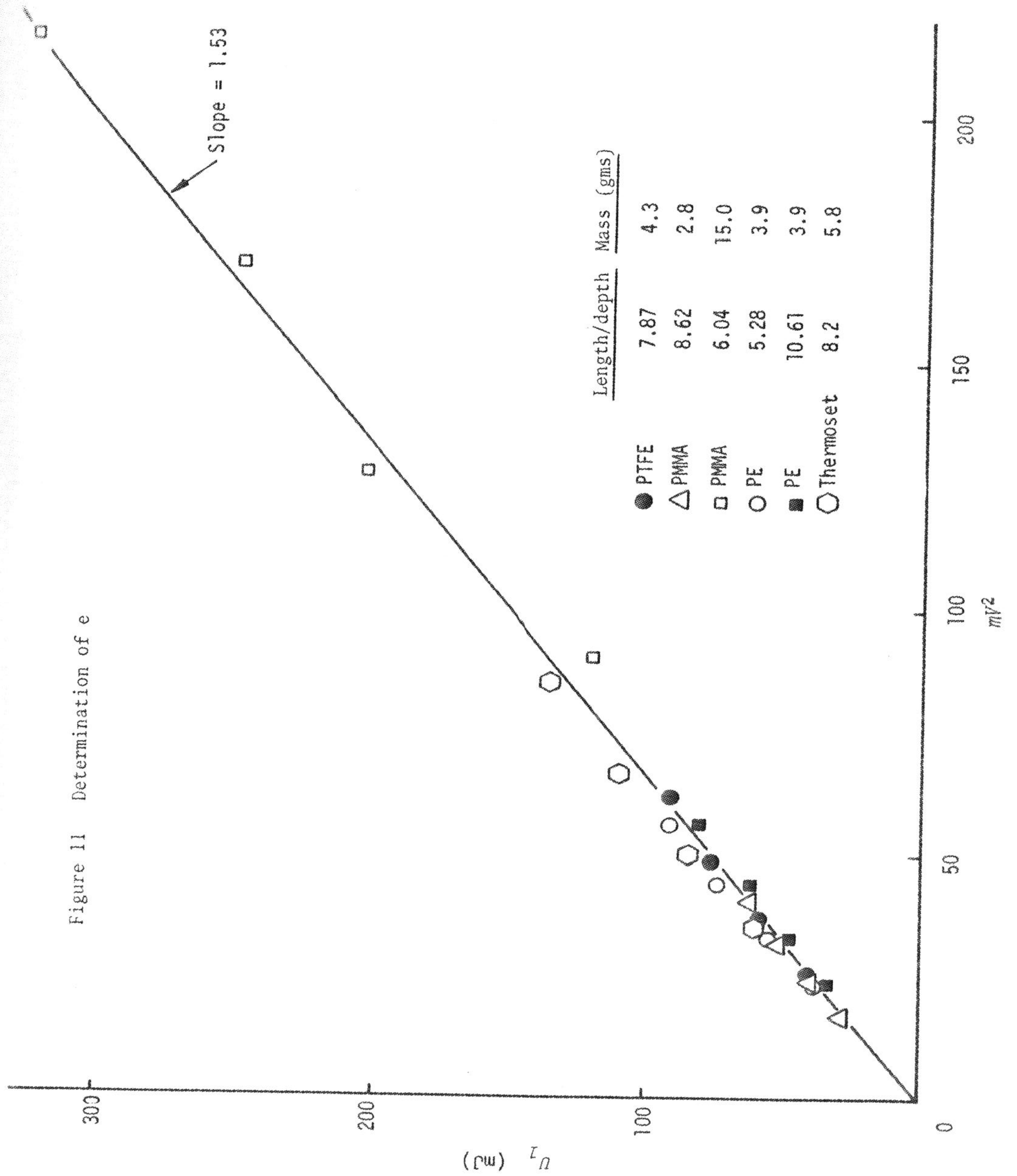

Figure 11 Determination of e

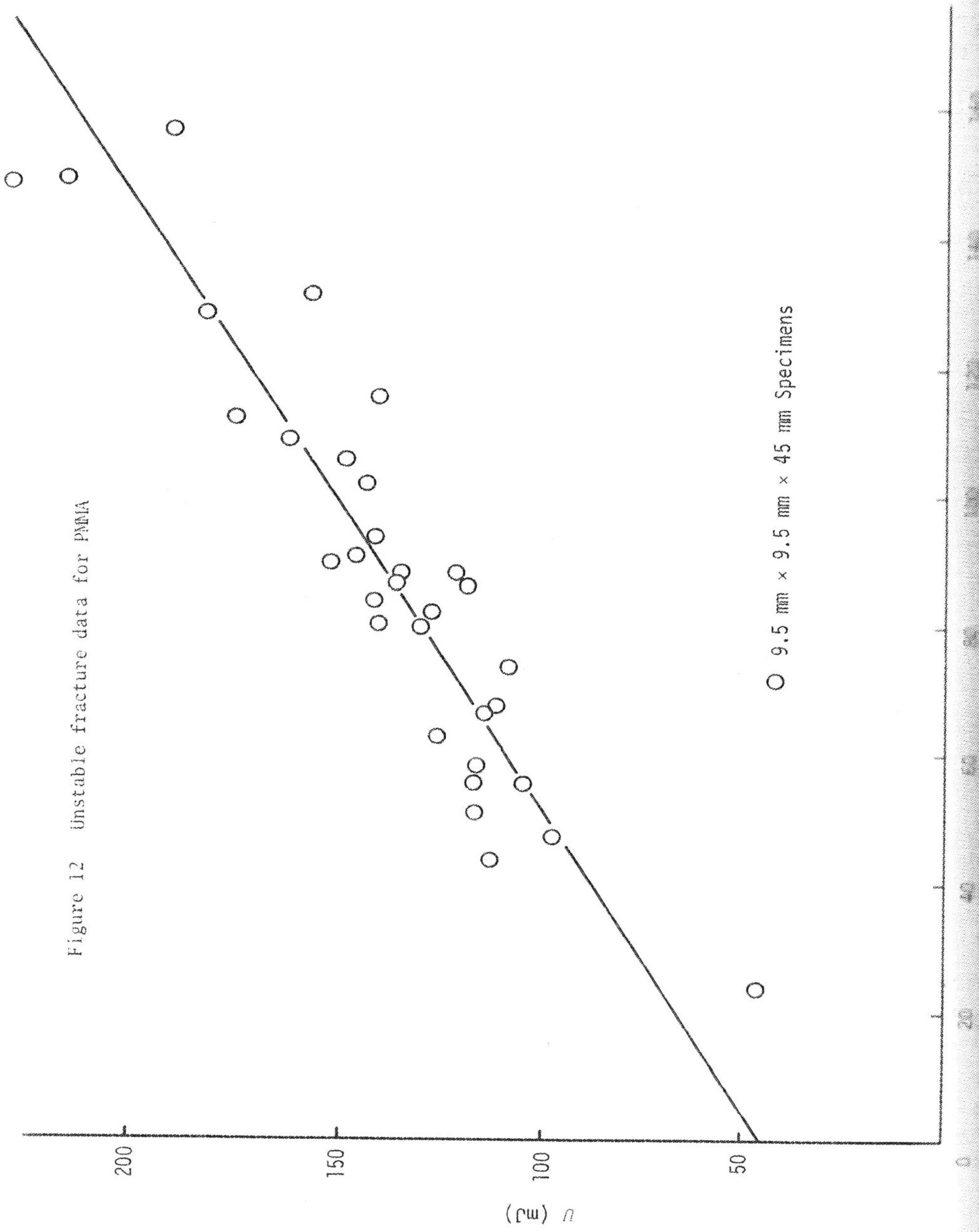

Figure 12 Unstable fracture data for PMMA

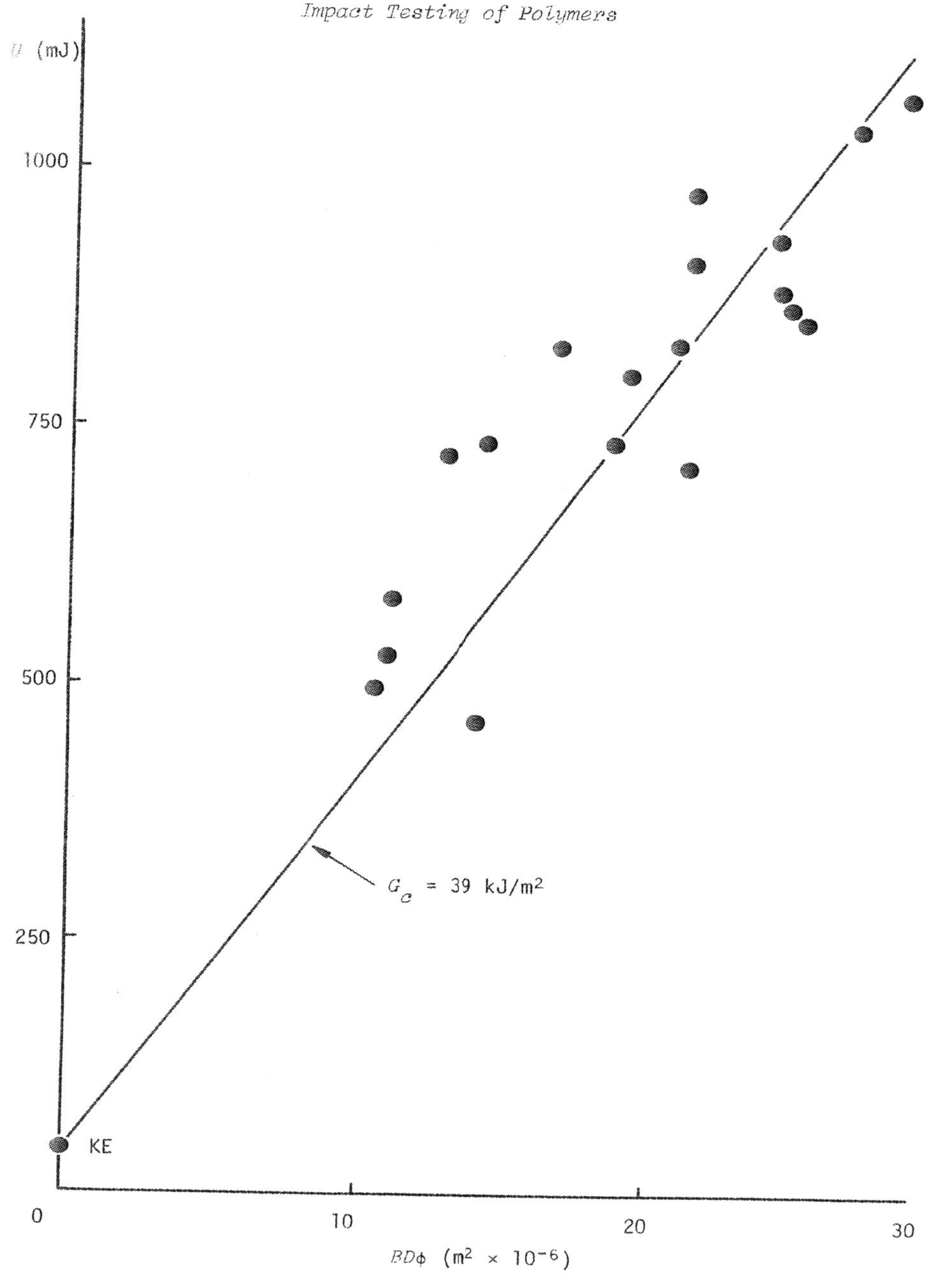

Figure 13 Unstable fracture in a glass fibre reinforced resin

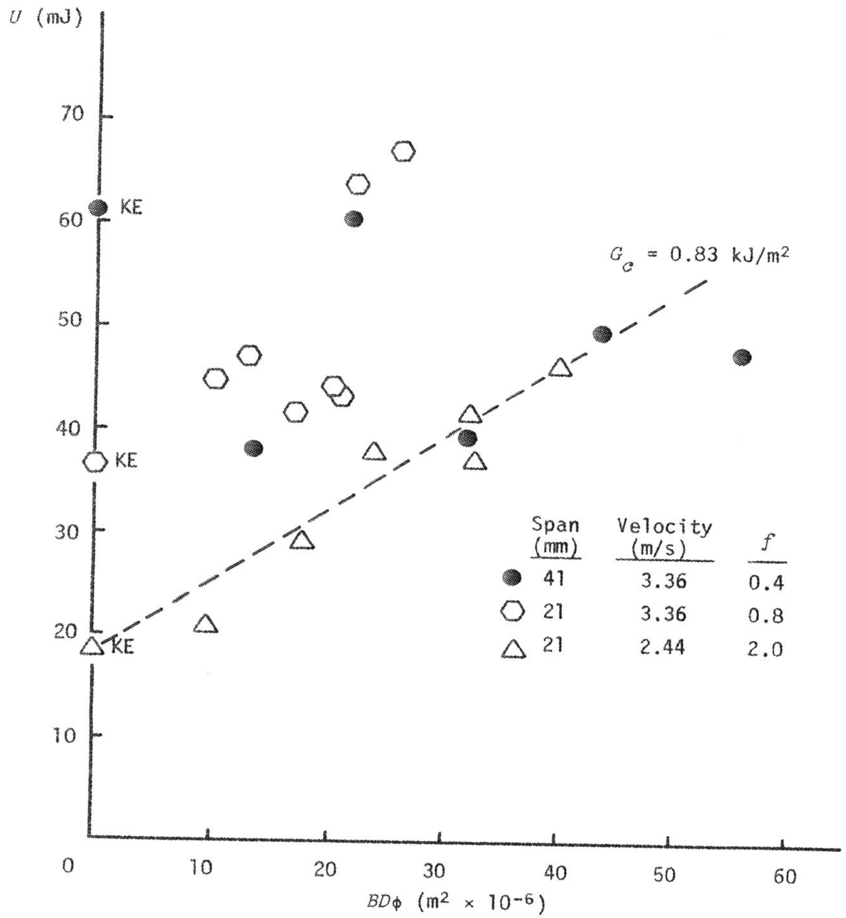

Figure 14 Unstable fractures in a low toughness moulding compound illustrating discrimination effects

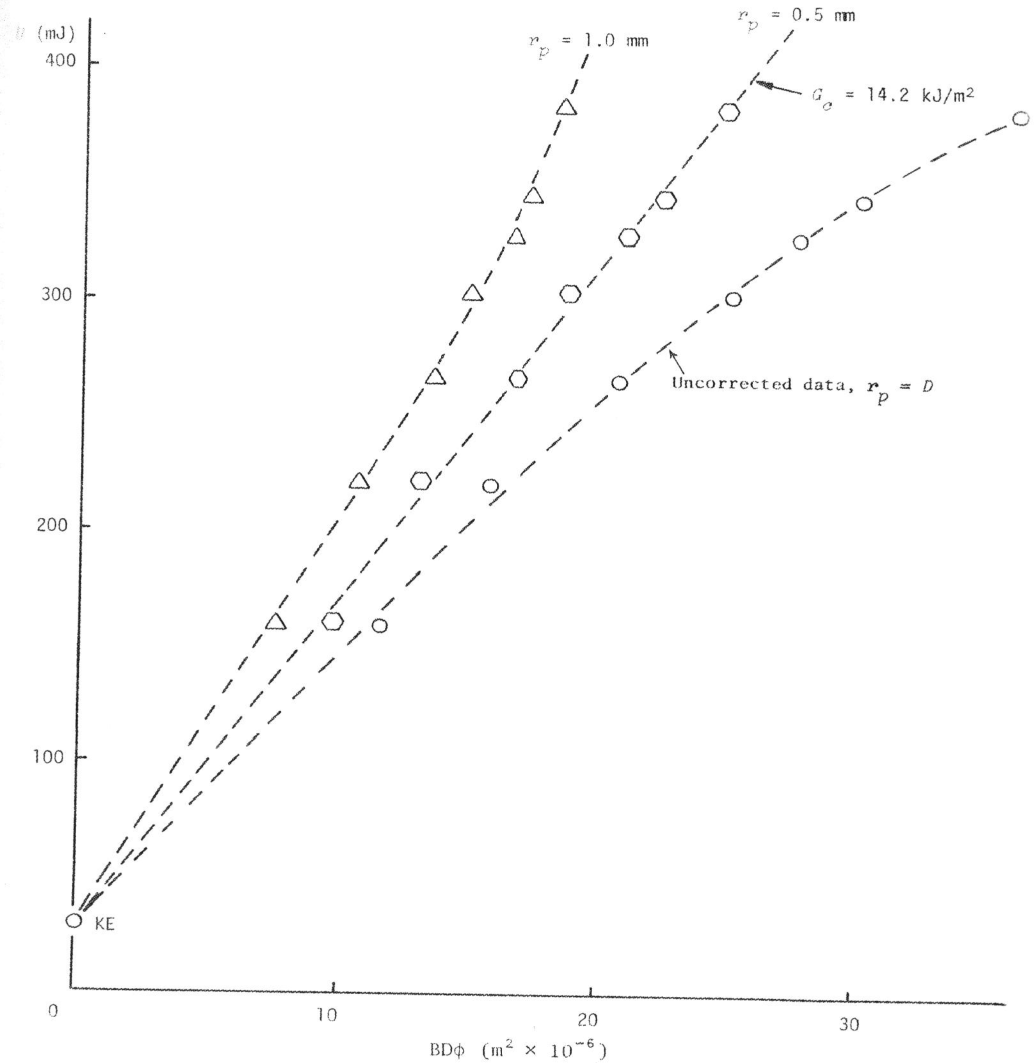

Figure 15 The effect of the plastic zone in medium density polyethylene data

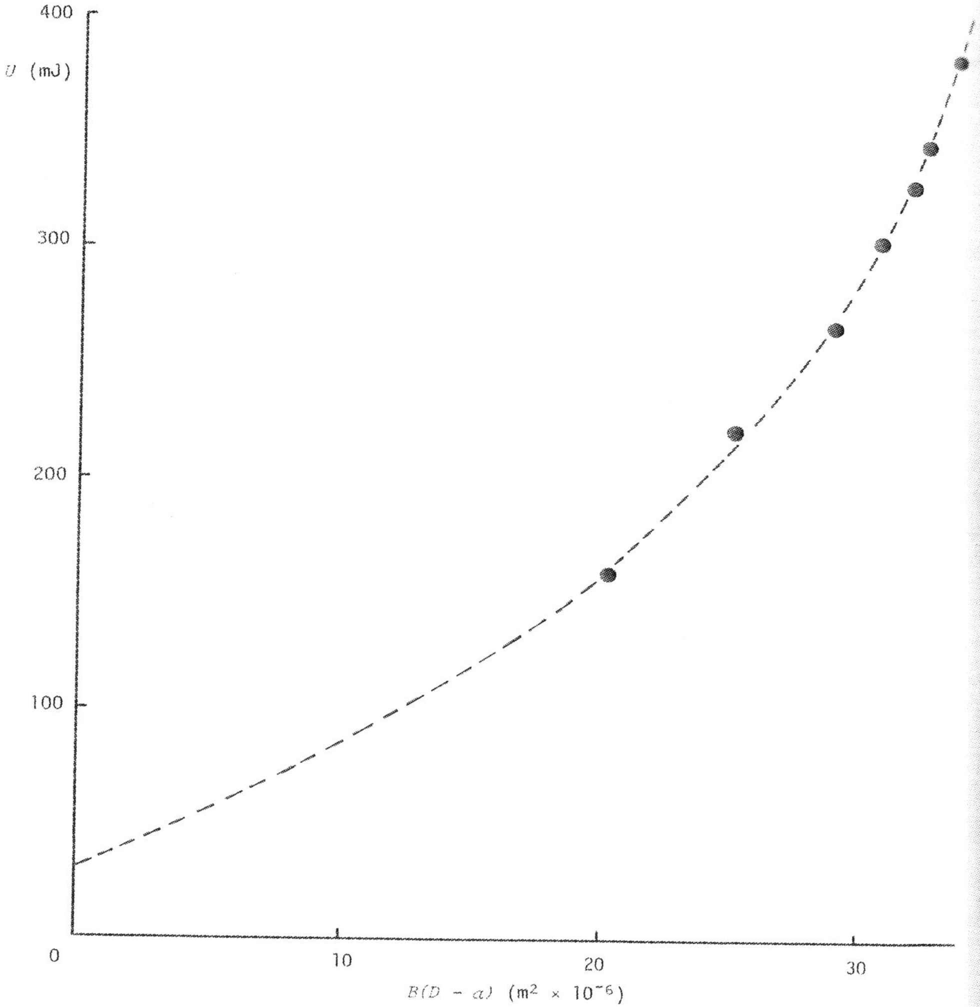

Figure 16 Low density polyethylene data plotted on a ligament area basis

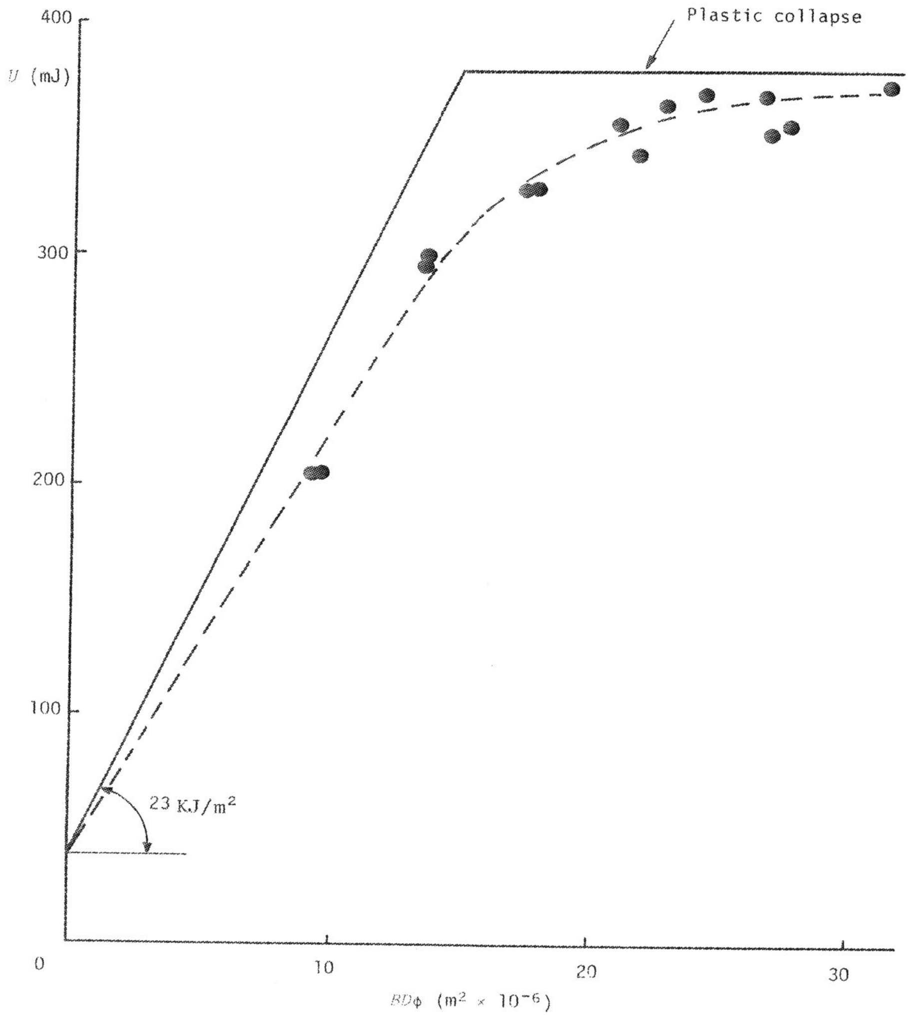

Figure 17 Pronounced plasticity effects for ABS

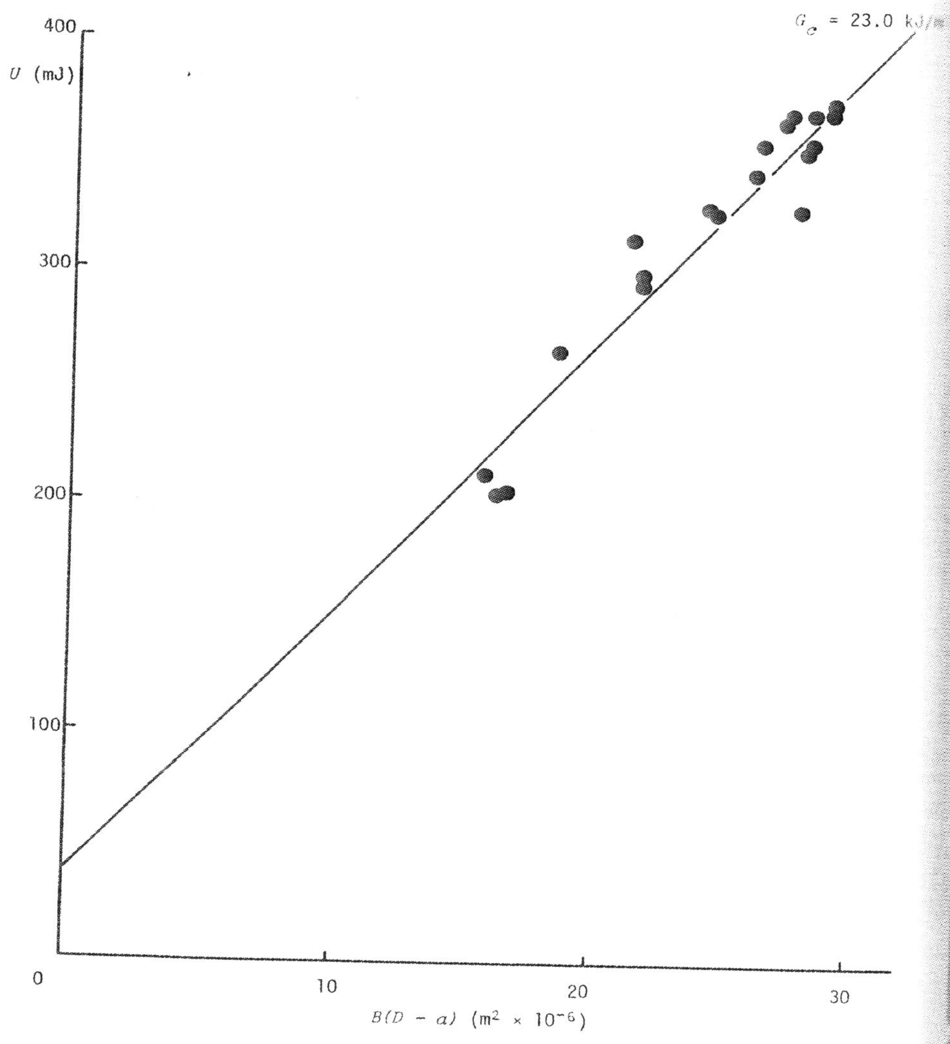

Figure 18 ABS data on a ligament area basis